Effects of Peripheral Planing on Surface Characteristics and Adhesion of a Waterborne Acrylic Coating to Black Spruce Wood

Julie Cool
Roger E. Hernández

Abstract

Peripheral planing of black spruce (*Picea mariana*) wood was optimized for rake angle and feed speed. Both cutting parameters affected surface characteristics at the microscopic and macroscopic level. In turn, the interaction between rake angle and feed speed had a significant impact on surface roughness, disperse component of surface energy, and total surface energy, as well as on initial pull-off adhesion strength of a waterborne coating. Loss in adhesion during the accelerated aging treatment was significantly lower for samples machined with a rake angle of 10°. This rake angle combined with a wavelength (feed per knife) of 1.3 mm yielded coated surfaces with high initial pull-off strength. Therefore, this wavelength could be used to increase production rates without significantly affecting surface quality. In addition, no torn grain was observed for surfaces prepared with a rake angle of 10° regardless of feed speed.

It is widely known that wood surface characteristics affect coating adhesion (Gindl et al. 2004, de Moura and Hernández 2005, Cool and Hernández 2011b). Because microstructure and chemical composition of wood surfaces are affected by the machining process (Murmanis et al. 1983, 1986; Gardner et al. 1991; de Moura et al. 2010), it is important to study its impact on wood coating adhesion. Peripheral planing is one of the most important wood machining processes; therefore, it is extensively studied (Williams and Morris 1998). It is largely recognized that feed speed is one of the most important cutting parameters when looking for improving surface quality. Reducing wavelength (feed per knife) by lowering feed speed improves surface quality (Koch 1972) by decreasing the normal cutting force component (Koch 1972, Carrano et al. 2004). Rake angle also has an important impact on surface quality, but sensitivity to rake angles (Koch 1985) and tool wear (Hernández and Naderi 2001, Hernández and de Moura 2002, Hernández and Rojas 2002) varies with wood species. As a result, optimal rake angles may vary from 5° to 25° depending on wood species and moisture content (Koch 1985). The standard ASTM D1666 (ASTM International 2004) may provide ground rules in initial selection of feed speed and rake angle (Cantin 1967, Williams and Morris 1998, Lihra and Ganev 1999). Moreover, machining with conventional planing often produces crushed cells and checks on the surface and subsurface (Stewart and Crist 1982). This damage could hinder varnish penetration in sugar maple (*Acer saccharum*) wood (de Moura and Hernández 2005). However, Hernández and Naderi (2001) suggested that permeability of heterogeneous woods, such as red oak (*Quercus rubra*) and white spruce (*Picea glauca*), could be increased by the compression force induced during cutting. As a result, gluing capability was enhanced for these woods.

Black spruce (*Picea mariana* (Mill.) BSP) is one of the most important boreal tree species in Canada. Its properties and abundance make it a valuable resource, and its wood is widely used in the pulp and paper industry and in construction applications such as lumber and glued structural members. This species has been included in general studies on Canadian woods undertaken by Lihra and Ganev (1999). Based on Standard ASTM D1666 (ASTM International 2004), cutting parameters for planing this wood were suggested when using a conventional peripheral

The authors are, respectively, Scientist, FPInnovations, Québec, Canada (julie.cool@fpinnovations.ca [corresponding author]); and Professor, Centre de recherche sur le bois, Département des sciences du bois et de la forêt, Univ. Laval, Québec, Canada (roger.hernandez@sbf.ulaval.ca). This paper was received for publication in January 2012. Article no. 12-00001.

Forest Prod. J. 62(2):124–133.

process. However, compared with other wood species, black spruce proved difficult to plane in a manner that produces defect-free surfaces. The numerous knots and grain deviation generated torn grain, while differences in density between earlywood and latewood brought raised grain. Although slight torn grain was observed, Cool and Hernández (2011a) recently reported that the peripheral planing process with a 12° rake angle and a wavelength of 1.67 mm induced good surfaces for mechanical adhesion of poly (vinyl acetate) glue. The large number of cell lumens available and the fibrillation appeared to favor penetration of adhesive and increase the surface available for its mechanical anchorage. The authors also reported the effect of machining with alternative planing processes (Cool and Hernández 2011b) and sanding (Cool and Hernández 2011c). Their results showed that oblique planing with an oblique angle of 35° produced surfaces without any damage and having opened tracheid lumens. This allowed the acrylic coating to penetrate in wood samples. However, oblique planing is a process occurring at quite low feed speeds. Optimizing machining parameters for the peripheral planing process, which is widely used in the wood industry, could further improve surface quality and adhesion. This could favor the use of black spruce wood for appearance purposes. Hence, this work evaluated the effect of feed speed and rake angle during the peripheral planing process on anatomy, surface roughness, wettability, and adhesion of a water-based coating on black spruce wood samples.

Materials and Methods

Testing materials

Black spruce wood was selected for this study. We kiln dried 270 flat sawn boards (860-mm length [L]) and stored them in a conditioning room at 20°C and 40 percent relative humidity (RH) until they reached 10 percent equilibrium moisture content (EMC). After conditioning, all sections were machined at 52-mm (tangential [T]) width and 22-mm (radial [R]) thickness. A 25-mm-long section was crosscut from each specimen to measure the average (455 kg/m^3) and standard deviation (35 kg/m^3) of basic density (ovendry mass over green volume). Specimens were then divided into nine groups having an average density of 455 kg/m^3 each. Subsequently, each group underwent a surfacing treatment. After surfacing, samples were resectioned to prepare specimens for roughness (50 mm [L]), microscopy (25.4 mm [L]), wettability (160 mm [L]), and coating application (620 mm [L]). After coating application, two matched samples were sawn. One sample underwent an accelerated aging treatment before being submitted to the adhesion test, and the other remained untreated for comparison purposes.

Machining treatments

Peripheral straight-edge knife planing was used to surface the specimens. Previous cuts were carried out to level samples and run-in knives prior to each surfacing treatment. Planing was performed with a Weining Powermat 1,000 moulder equipped with a cutterhead having 53 mm of cutting radius. The cutterhead rotation speed was 10,000 rpm with three different feed speeds, 8, 10, and 13 m/min. This produced 0.8-, 1.0-, and 1.3-mm wavelengths, respectively. These wavelengths are small and usually recommended for finishing purposes. Hence, planing should result in good surface quality. Cutting depth was 1 mm, and three rake angles were studied (10°, 15°, and 20°). The clearance angle was kept constant at 20° for all three rake angles.

Microscopic evaluation

Ten-millimeter cubes were cut to observe tangential and end-grain surfaces. Tangential surfaces were used to evaluate the fibrillation level and open lumens. End-grain surfaces were used to analyze cell damage and coating penetration. One end-grain surface was carefully cut with a razor blade mounted onto a microtome. All cubes were then desiccated with phosphorous pentoxide (P_2O_5) for a week and mounted on standard aluminum stubs with silver paint. Environmental scanning electron microscopy micrographs were taken for two representative machined samples for each machining treatment.

Surface topography measurements

Roughness measurements were carried out on defect-free zones with a Micromeasure confocal microscope. A surface of 12.5 mm (L) by 12.5 mm (T) was analyzed for each sample. Data were collected with Surface Map 2.4.13 software using an acquisition frequency of 300 Hz and a scanning speed of 12.5 mm/s. Three-dimensional roughness parameters were determined using the Mountain software. A cutoff length of 2.5 mm combined with a Robust Gaussian filter (ISO 16610-31; International Organization for Standardization 2002) were used for calculations. Arithmetical mean deviation of the profile (S_A), maximum profile peak height (S_P), and maximum profile valley depth (S_V) were calculated according to ISO 4287 (ISO 1997). Core roughness depth (S_K), reduced peak height (S_{PK}), and reduced valley depth (S_{VK}) were calculated from the Abbot curve according to ISO 13565-2 (ISO 1996).

Wettability measurements

Wetting properties were evaluated within 8 hours following the machining treatments. Wetting analyses were performed with a FTÅ D200 imaging goniometer at 20°C. One drop (~6 μL) of pure water was added to wood surfaces with an injection microsyringe. A frame grabber recorded changes in droplet profile during the first 120 seconds of wetting. The measurements were carried out fiberwise because wetting is more important and constant in this direction (Gardner et al. 1991, de Meijer et al. 2000). Contact angle was calculated as a mean of both sides of the drop in order to compensate for any horizontal variations. Wetting rate was calculated as $\Delta\theta/\Delta t$ to assess spreading and penetration of pure water over the first 30 seconds of wetting. For surface energy measurements, initial contact angle of formamide was measured. Nonpolar and polar components of the surface energy were calculated using the harmonic mean method according to Wu (1971). According to Piao et al. (2010), no procedure has been developed for determining absolute values of surface energy. However, several authors have used this method to describe physicochemical changes of wood surfaces produced by different treatments (Wang et al. 2007, Wolkenhauer et al. 2007).

Coating application procedure

Machined surfaces were coated within 8 hours after the machining treatments. During this period, samples were

placed face against face in order to keep contamination at minimum levels. Two coats of an acrylic water-based coating Laurentide–Innocryl PF were air sprayed (150-μm wet thickness) at room temperature according to manufacturer's specifications. Coating was then cured in an infrared oven following a methodology established with the coating manufacturer.

Accelerated aging

One set of specimens underwent accelerated aging treatments in a Cincinnati SubZero environmental stimulation chamber (WM-906-MP2H-3-SC/WC) with temperature and RH precisions of ±1°C and ±3 percent, respectively. Treatment was based upon ASTM D3459 (American Society for Testing and Materials 1998) and consisted of four cycles of 48 hours at 50°C and 10 percent RH followed by 48 hours at 50°C and 90 percent RH. Prior to treatment, specimen ends were sealed with paraffin to reduce moisture exchange through cross section. After aging, specimens were conditioned at 20°C and 40 percent RH until they reached their initial EMC (10%).

Adhesion tests

Adhesion of aged and unaged films was evaluated by means of a pull-off test according to ASTM D4541 (ASTM International 2002). A MTS QT5 universal testing machine having a maximal load capacity of 5 kN and ±0.12 percent precision was used. Small 20-mm-diameter dollies were glued on the film surface with Araldite 2011 two-part epoxy resin. After 24 hours of curing at 20°C and 40 percent RH, the perimeters of glued dollies were carefully incised to prevent propagation of failures out of the tested area. Pulling was applied at 1 mm/min until separation of the dolly from the substrate. Maximal normal pull strength at rupture was recorded.

Statistical analyses

A factorial design with two factors, feed speed and rake angle, was established for the experiment. Data followed a randomized block design, and results from mechanical tests were analyzed with the mixed procedure in SAS as repeated measures. Surface topography, wettability, and surface energy were analyzed as a one-way analysis of variance, following the general linear model procedure. Mean difference comparison tests were performed at a 5 percent probability level when required. Simple correlations between surface quality parameters and the pull-off results were studied using the correlation procedure. Analysis was done on SAS statistical package, version 9.2 (SAS Institute Inc. 2007).

Results and Discussion

Microscopy

End-grain surfaces.—Peripheral planing treatments used in this experiment induced slight subsurface damage in black spruce wood surfaces. When it occurred, damage was limited to the first row of cells in both earlywood and latewood (Figs. 1 through 3). Few differences were observed among samples planed with 10° and 15° rake angles regardless of feed speed (Figs. 1 and 2). However, samples planed at a 20° rake angle seemed to have suffered more damage when the wavelength was larger than 0.8 mm (Fig. 3). The waterborne coating did not penetrate into cells.

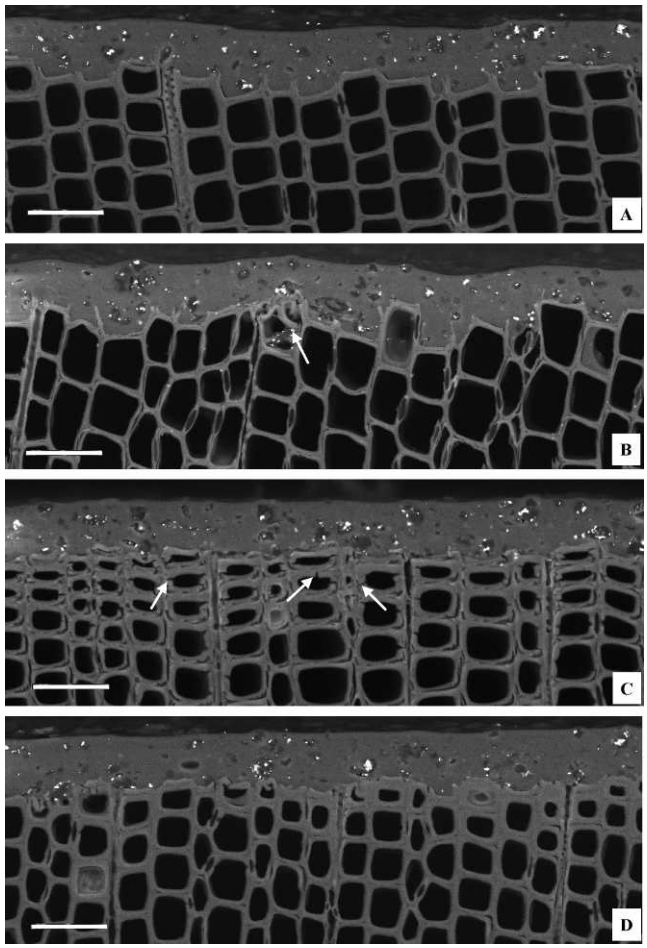

Figure 1.—Transverse environmental scanning electron microscopy micrographs of earlywood (A and B) and latewood (C and D) black spruce wood samples planed with a rake angle of 10°. Arrows show deformed cells in B and C as well as microruptures in C. Scale bars = 50 μm.

This is in agreement with previous scanning electron microscopy observations of the interface of acrylic coatings and wood surfaces (Thay and Evans 1998). It only filled lumens that were available on the surface after planing. Because of its higher radial diameter, more lumens were available in earlywood than in latewood (de Moura et al. 2010). Cutting action occurred more in latewood, and failures, in that case, often took place in or close to the middle lamella. Consequently, filling of lumens by the coating was lower in latewood than in earlywood areas (Figs. 1 through 3).

Specimens planed with a rake angle of 10° and 15° were similar and characterized by superficial subsurface damage (Figs. 1 and 2), comparable with what was reported for peripheral-planed black spruce wood with a 12° rake angle (Cool and Hernández 2011a). However, little crushing, more or less severe, was locally observed in earlywood (Fig. 1B) and in latewood (Fig. 2B). In some areas, cell walls in latewood showed microruptures (Fig. 1C). These microruptures, as well as slight crushing, were only observed in samples planed with a rake angle of 10°. Given that normal cutting force is of compressive nature throughout the visible part of the cutting path (Iskra and Hernández 2012), and because Type III chips are probably produced with low rake

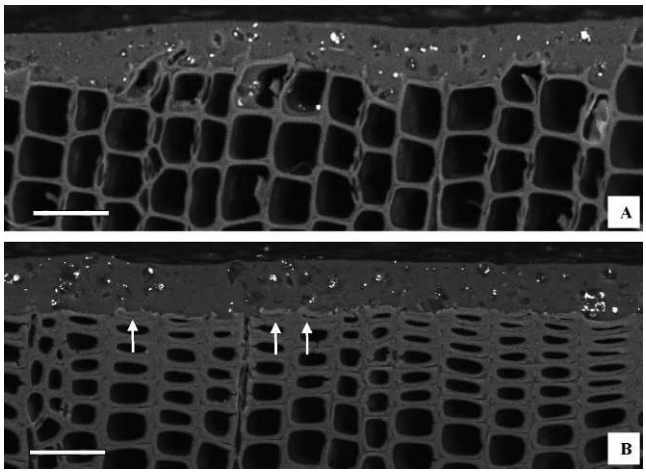

Figure 2.—Transverse environmental scanning electron microscopy micrographs of earlywood (A) and latewood (B) black spruce wood samples planed with a rake angle of 15°. Arrows show deformed cells in latewood (B). Scale bars = 50 μm.

angles in peripheral up-milling (Koch 1985), it can be assumed that lower rake angles could compress cells to a greater extent. As a result, samples showed occasional slight crushing and microruptures, which were not seen in samples planed with a 15° rake angle.

Samples planed with a rake angle of 20° and a wavelength of 0.8 mm were virtually free of subsurface damage (Fig. 3A). When wavelength increased to 1.0 and 1.3 mm, slight crushing was induced in earlywood (Figs. 3B and 3C) and latewood (Fig. 3D) areas. According to Singh et al. (2010), deformed cells can be observed even though cell walls appear to be intact. With a rake angle of 20°, a Type II chip should be principally induced in the visible part of the cutting path (Koch 1985). As wavelength increases, Iskra and Hernández (2012) reported little effect on the negative normal force component, responsible for cell deformation and crushing, in peripheral up-milling of sugar maple wood. However, increasing wavelength had an impact on the parallel force component. The resulting cutting force could partially be responsible for the observed cell damage. However, subsurface damage at these conditions was very slight and still lower than that reported for face-milled (Cool and Hernández 2011b) or sanded surfaces machined with a single-stage program (Cool and Hernández 2011c).

Tangential surfaces.—All surfaces were characterized by open lumens of tracheids and rays, plateau-like areas, and fibrillation. The availability of lumens should favor filling and coating penetration and increase mechanical anchorage of coating (Figs. 4 through 6; Singh and Dawson 2004, 2006). Fibrillation should also increase coating mechanical anchorage. According to micrographs, little effect of the feed speed could be observed, whereas the rake angle had a higher impact on the planed surfaces.

At 10° rake angle, feed speed had little effect on tangential surfaces. Regardless of feed speed, surfaces showed low fibrillation, which corresponded to torn portions of tracheid cell walls (Figs. 4A, 5A, and 6A). Plateau-like regions, similar to those obtained by oblique cutting and helical planing of black spruce (Cool and Hernández 2011b) and by oblique cutting of sugar maple (de Moura and Hernández 2007), red oak, and white pine (*Pinus strobus*) wood (de Moura et al. 2010), were also observed. As

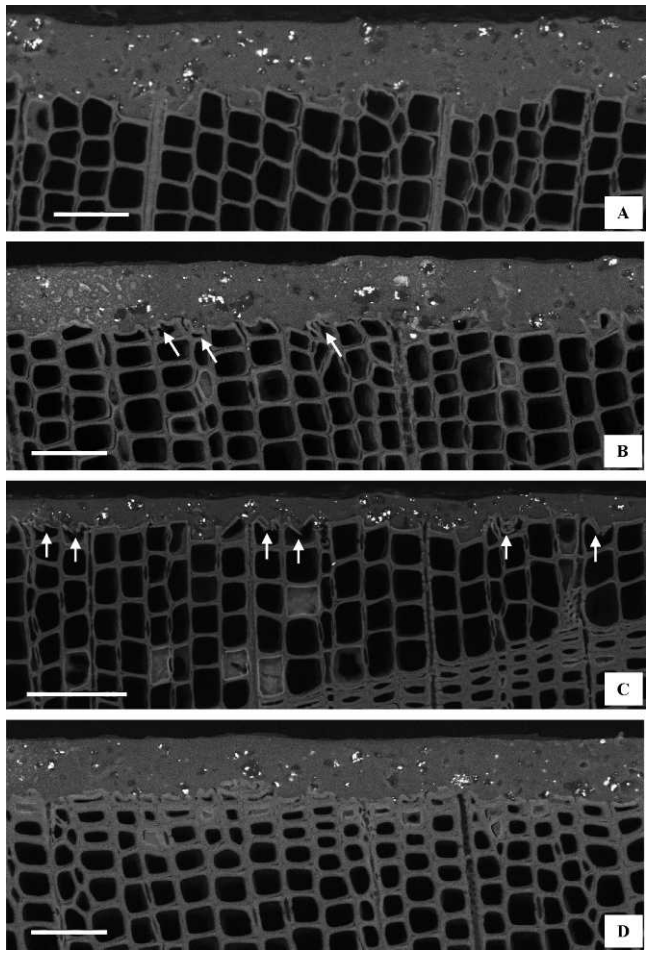

Figure 3.—Transverse environmental scanning electron microscopy micrograph of black spruce earlywood planed with a rake angle of 20° and a wavelength of 0.8 mm (A), 1.0 mm (B), and 1.3 mm (C), as well as latewood planed with a wavelength of 1.0 mm (D). Arrows show slight subsurface damage in earlywood. Scale bars = 50 μm for A, B, and D and 100 μm for C.

reported by de Moura et al. (2010) for oblique-cut surfaces, the cutting action in peripheral planing took place by peeling in or close to the middle lamella. Ashby et al. (1985) reported similar results with various woods when studying crack propagation in the same cutting plane of this study (radial–longitudinal plane).

As rake angle was increased to 15°, the fibrillation for surfaces prepared with a wavelength of 0.8 mm was similar to that observed on specimens planed with a rake angle of 10° (Figs. 4A, 4B, 5A, and 6A). As wavelength was increased to 1.0 and 1.3 mm, fibrillation increased (Figs. 5B and 6B). However, little subsurface damage was observed in end-grain surfaces (Fig. 2). Consequently, the resulting surface quality was probably associated with formation of chip Types II and III. Because surface quality was similar for samples planed with a wavelength of 0.8 mm, the cutting action (chip formation) was probably the same as that of samples prepared with a 10° rake angle. However, increasing wavelength could have increased cutting forces and slightly modified the cutting action. Hence, it took place through cell walls, and it amplified fibrillation levels slightly.

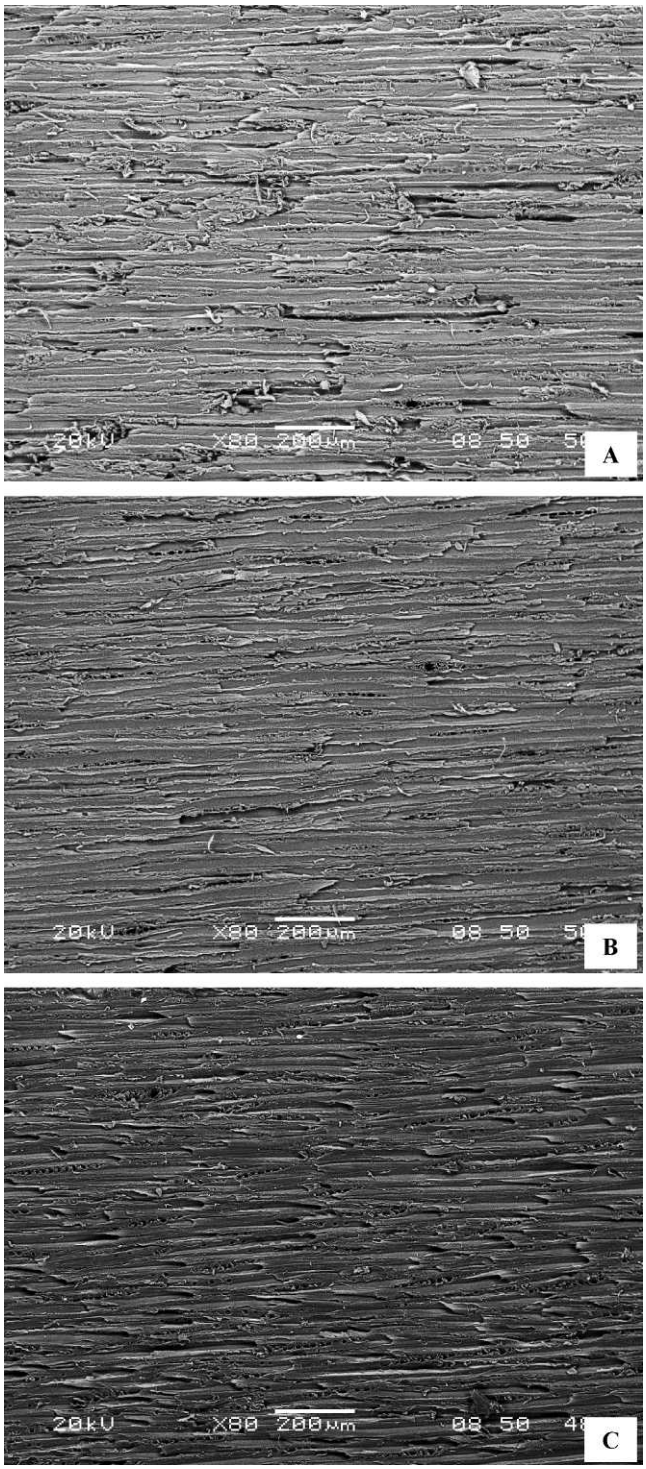

Figure 4.—Tangential environmental scanning electron microscopy micrographs of black spruce wood samples that were planed at a wavelength of 0.8 mm with a rake angle of 10° (A), 15° (B), and 20° (C).

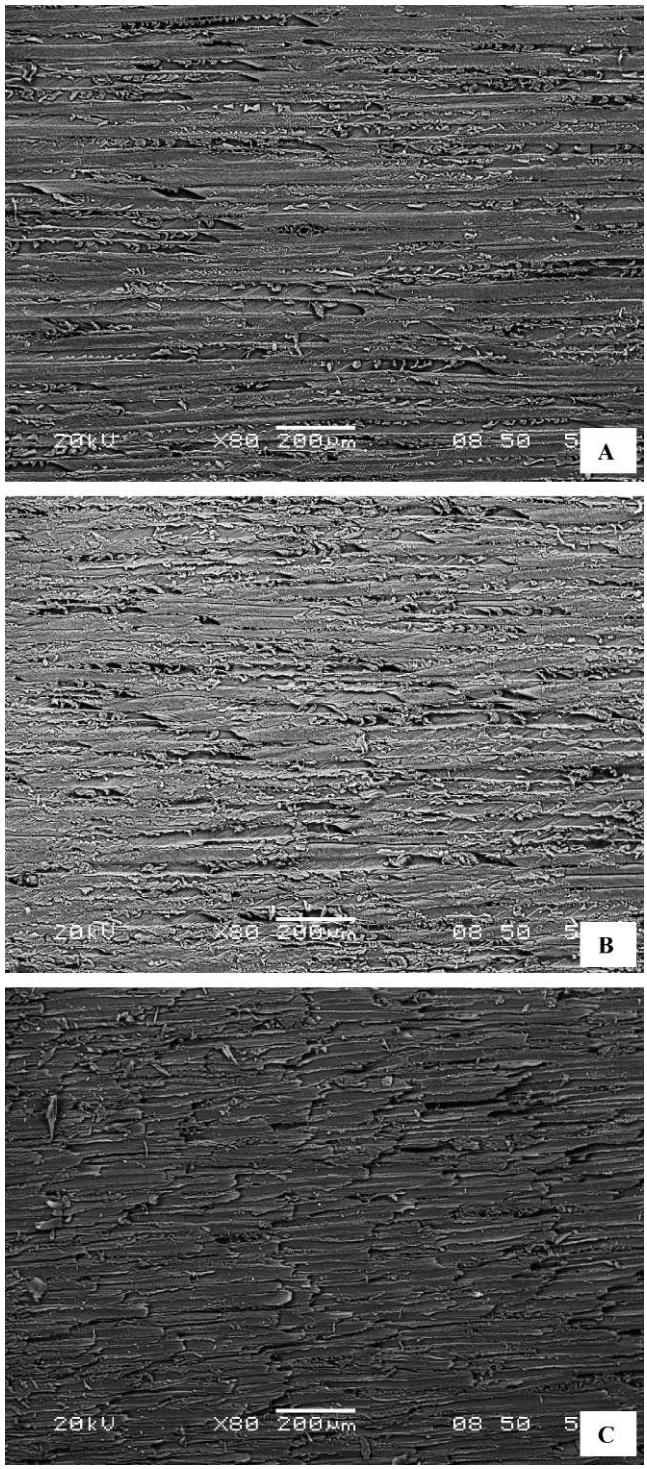

Figure 5.—Tangential environmental scanning electron microscopy micrographs of black spruce wood samples that were planed at a wavelength of 1.0 mm with a rake angle of 10° (A), 15° (B), and 20° (C).

When planing with a rake angle of 20°, fibrillation was reduced, but an important level of tearing appeared (Figs. 4C and 5C) with wavelengths of 0.8 and 1.0 mm. This tearing could be associated with Type I chip formation, which is favored when a knife is traveling on local grain deviation areas (against the grain milling). As wavelengths reached 1.3 mm, the normal cutting force is increased, and slight crushing (Figs. 3B through 3D) as well as plateau-like regions were visible on the surfaces (Fig. 6C). These surfaces were similar to those planed with a rake angle of 10° as well as those planed with a rake angle of 15° with a wavelength of 0.8 mm. It appears that increasing the rake angle to 20° modified the cutting action of the knife. Planing still occurred by peeling in or close to the middle lamella,

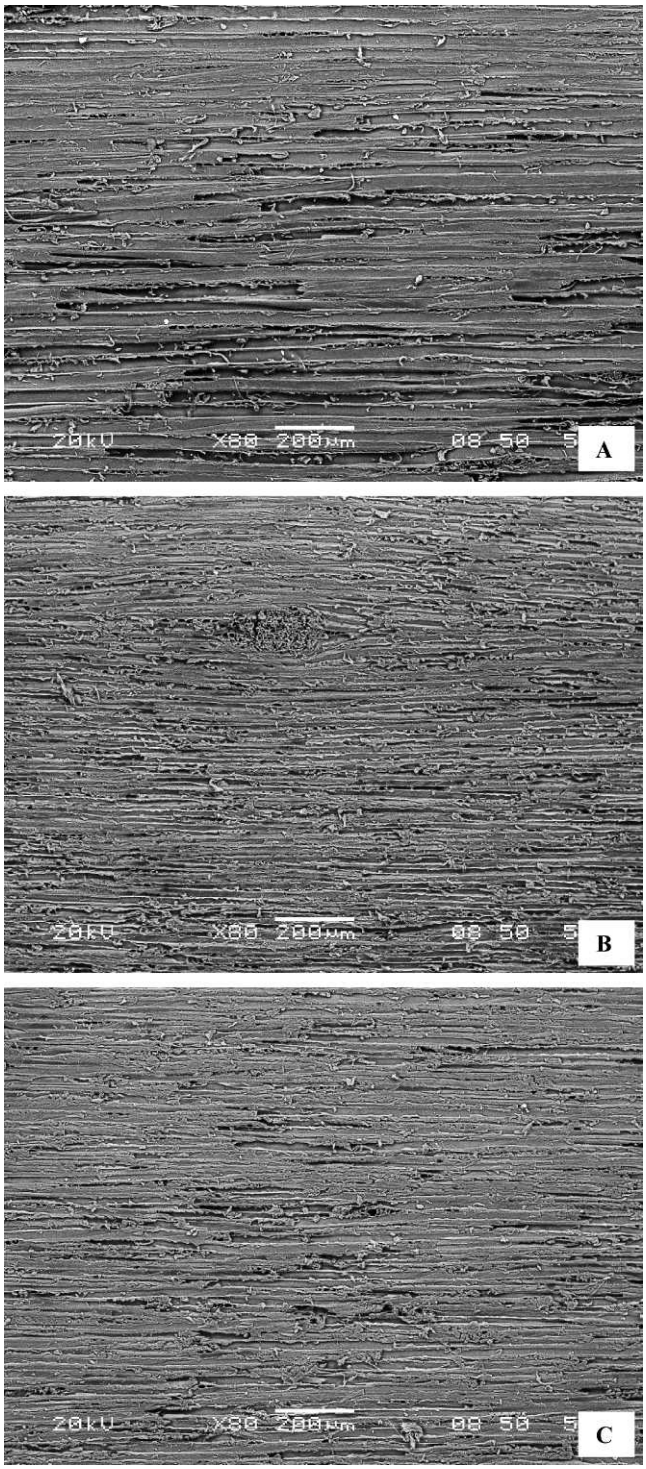

Figure 6.—Tangential environmental scanning electron microscopy micrographs of black spruce wood samples that were planed at a wavelength of 1.3 mm with a rake angle of 10° (A), 15° (B), and 20° (C).

but microruptures or cracks developed and extended below the surface, as does a Type I chip. As a result, surfaces were characterized by a certain level of tearing.

Information gathered from micrographs indicates that surface features depend on the cutting parameters. More specifically, cutting action and chip formation could change with rake angle and feed speed and affect surface quality at the microscopic level.

Surface roughness.—Slightly torn grain was observed near the knots in the samples planed with a rake angle of 15° and a wavelength of 1.3 mm and a rake angle of 20° with wavelengths of 1.0 and 1.3 mm. Previous authors have reported similar results when planing white spruce wood (Cantin 1967, Hernández et al. 2001). Based on ASTM D1666 (ASTM International 2004), these authors concluded that a higher proportion of defect-free surfaces was obtained at a 15° rake angle with a wavelength of 1.3 mm. However, Hernández et al. (2001) observed that torn grain was less important in samples planed with a 10° rake angle, even though the presence of fuzzy grain increased. Because wood density of black spruce wood is higher than that of white spruce wood (Jessome 1977) and studied wavelengths were equal to 1.3 mm or smaller, the impact of the rake angle on the occurrence of surface defects was diminished.

Feed speed and rake angle both had a significant effect on four surface roughness parameters, S_A, S_P, S_K, and S_{PK}, but not on S_V and S_{VK}, where no significant differences were detected between treatments (Table 1). The four roughness parameters were also significantly affected by the interaction between rake angle and feed speed. In agreement with observations made from Figures 4 through 6, rake angle appeared to affect surface roughness more. For S_A and S_K, smoother surfaces were obtained when using a rake angle of 20° with a wavelength of 1.0 or 1.3 mm and a rake angle of 15° with a wavelength of 0.8 mm. The lower fibrillation observed on these surfaces contributed to significantly minimize surface roughness (Figs. 4 through 6; Table 1). These samples were also characterized by plateau-like regions, which further reduced S_A and S_K.

The parameters S_P and S_{PK} both give information on peaks in the surface roughness profile. More specifically, S_{PK} was often related to fuzzy grain (Fujiwara et al. 2005, Gurau et al. 2005) or to the level of fibrillation (Cool and Hernández 2011a, 2011b, 2011c). Because none of the samples were characterized by fuzzy grain, S_{PK} could be related to the fibrillation levels observed in samples. According to Table 1, values of S_P and S_{PK} were lower for surfaces planed with a rake angle of 20° at wavelengths of 1.0 and 1.3 mm and for those planed with rake angles of 10° and 15° at a wavelength of 0.8 mm. These samples were characterized by smooth areas with low fibrillation levels (Figs. 4 through 6), which contributed to the decrease of both S_P and S_{PK} parameters.

Wettability tests

No effect of machining parameters was detected on measured contact angle or the spreading and penetration of oopure water (Fig. 7). However, machining parameters had a significant effect on surface energy (Tables 2 and 3). The nonpolar or disperse component of the surface energy was significantly affected by the interaction between rake angle and feed speed (Table 2). Smaller values were observed for surfaces machined with a rake angle of 20° at wavelengths of 1.0 and 1.3 mm, whereas the best value was obtained at this rake angle but at a wavelength of 0.8 mm. Consequently, more sites were available to form hydrogen bonds with the waterborne coating on the latter surfaces. Lower normal cutting force associated with shorter wavelengths could have generated less heat, which reduced surface inactivation compared with higher feed speeds. Polar component was

Table 1.—Three-dimensional surface roughness parameters (μm) of black spruce wood specimens prepared by peripheral planing at three rake angles and wavelengths.[a]

Rake angle (°)	Wavelength (mm)	S_A	S_K	S_P	S_V	S_{PK}	S_{VK}
10	0.8	6.9 (0.3) D	20.0 (1.0) D	30.1 (1.5) AB	37.3 (1.7)	8.2 (0.5) ABC	12.3 (0.6)
	1.0	6.9 (0.2) CD	19.6 (0.7) CD	32.5 (1.3) B	35.3 (1.1)	9.9 (0.6) D	11.8 (0.4)
	1.3	6.9 (0.3) CD	19.7 (0.9) CD	34.0 (1.8) B	34.5 (1.6)	10.3 (0.7) D	11.3 (0.5)
15	0.8	6.2 (0.2) ABC	17.2 (0.6) AB	30.6 (1.3) AB	33.7 (1.2)	9.2 (0.5) BCD	11.3 (0.4)
	1.0	6.8 (0.3) BCD	19.5 (0.9) CD	32.7 (1.8) B	35.3 (1.9)	9.3 (0.6) BCD	11.5 (0.6)
	1.3	6.7 (0.2) BCD	19.1 (0.7) BCD	32.7 (1.5) B	33.5 (1.3)	9.7 (0.6) CD	11.1 (0.4)
20	0.8	6.7 (0.3) BCD	19.0 (0.9) BCD	33.7 (3.2) B	36.9 (2.6)	9.7 (1.0) CD	11.8 (0.5)
	1.0	5.5 (0.2) A	15.6 (0.5) A	27.3 (0.9) A	31.2 (1.3)	7.7 (0.3) AB	10.2 (0.5)
	1.3	6.1 (0.2) AB	17.6 (0.6) ABC	26.8 (1.1) A	35.1 (1.2)	7.1 (0.4) A	11.4 (0.5)

[a] Values are means (standard errors of the means) of 30 replicates. Means within a column followed by the same letter are not significantly different at the 5 percent probability level. S_A = arithmetical mean deviation of the profile; S_K = core roughness depth; S_P = maximum profile peak height; S_V = maximum profile valley depth; S_{PK} = reducd peak height; S_{VK} = reduced valley depth.

significantly affected by rake angle and feed speed. However, the interaction between both cutting parameters was not statistically significant. Thus, mean comparisons were performed separately for each source of variation by pooling values of the other source of variation (Table 3). This table shows that a rake angle of 20° and a wavelength higher than 0.8 mm significantly increased the polar component of surface energy. As reported by Gindl et al. (2004), a more important polar component is related to more hydrophilic surfaces. Although a rake angle of 20° and wavelengths of 1.0 and 1.3 mm resulted in a high polar component, the disperse component was lower for these cutting parameters (Table 2). The total surface energy had a similar behavior to the disperse component (Table 2). As for the latter, the former is significantly higher for surfaces planed with a rake angle of 20° at 0.8-mm wavelength. This shows that the total surface energy is strongly influenced by the disperse component of surface energy.

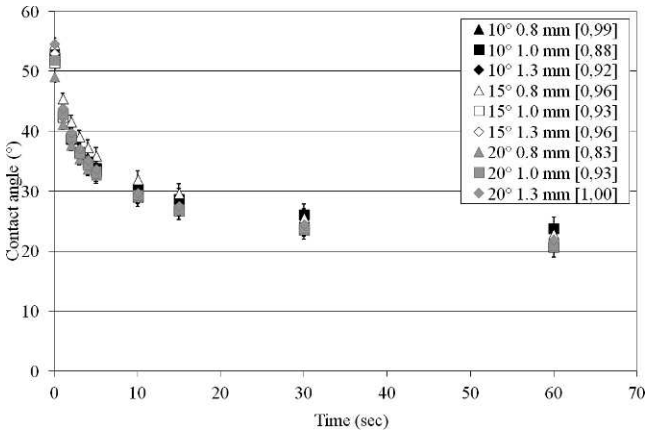

Figure 7.—Progression of the contact angle of a drop of pure water on black spruce wood samples planed with three rake angles and three wavelengths. For every planing condition, mean value of the wetting rate is in brackets.

Adhesion tests

Results of the pull-off tests are summarized in Table 4. Before aging, the interaction of feed speed and rake angle had a significant effect on pull-off strength. Based on these results, samples planed with a rake angle of 10° and a wavelength of 1.3 mm, a rake angle of 15° and wavelengths above 0.8 mm, and a rake angle of 20° and a wavelength of 0.8 mm had the highest pull-off strengths (Table 4). Pull-off strengths of planed samples were similar to those of sanded black spruce wood samples (Cool and Hernández 2011c). As mentioned previously, planed surfaces presented some fibrillation that could increase surface roughness (Figs. 4 through 6; Table 1). Therefore, mechanical adhesion was significantly favored. The chemical adhesion could also

Table 2.—Surface energy components determined by the harmonic mean method for black spruce wood specimens prepared by peripheral planing with three rake angles and wavelengths.

Rake angle (°)	Wavelength (mm)	Surface energy (mJ/m^2)[a]		
		Disperse	Polar	Total
10	0.8	18.1 (0.3) CD	30.1 (0.5)	48.2 (0.4) CDE
	1.0	19.3 (0.5) B	30.4 (1.0)	49.8 (0.9) BCD
	1.3	18.4 (0.3) BCD	31.3 (0.8)	49.7 (0.7) BC
15	0.8	17.9 (0.4) D	30.0 (0.5)	47.9 (0.5) DE
	1.0	18.0 (0.3) D	32.0 (0.6)	50.0 (0.6) B
	1.3	19.1 (0.4) BC	30.2 (0.5)	49.3 (0.4) BC
20	0.8	21.5 (0.4) A	31.0 (0.8)	52.5 (0.6) A
	1.0	16.1 (0.4) E	33.4 (0.6)	49.5 (0.5) B
	1.3	15.3 (0.4) E	32.2 (0.7)	47.5 (0.6) E

[a] Values are means (standard errors of the means) of 30 replicates. Means within a column followed by the same letter are not significantly different at the 5 percent probability level.

Table 3.—Results of the mean difference comparison tests performed on the data of the polar component of surface energy determined by the harmonic mean method for black spruce wood specimens prepared by peripheral planing at three rake angles and three wavelengths.

	Polar component (mJ/m^2)[a]
Rake angle (°)[b]	
10	30.6 (0.4) B
15	30.7 (0.3) B
20	32.2 (0.4) A
Wavelength (mm)[c]	
0.8	30.4 (0.4) B
1.0	31.9 (0.4) A
1.3	31.2 (0.4) AB

[a] Values are means (standard errors of the means) of 90 replicates. Means followed by the same letter are not significantly different at the 5 percent probability level.
[b] Wavelength values pooled.
[c] Rake angle values pooled.

have been improved for the samples prepared with a 20° rake angle through an increase in disperse and polar components of surface energy (Tables 2 and 3). During accelerated aging treatment, pull-off strength was significantly reduced by about 20 percent (Table 4). This behavior is similar to that observed by Cool and Hernández (2011b) on coated black spruce wood samples machined with alternative processes. However, after aging, water-based coating adhesion was not affected by either feed speed or rake angle. Furthermore, there were no statistically significant correlations between pull-off strength and the surface quality parameters (roughness and wettability) that were evaluated. Therefore, the pull-off strength test is required to assess coating performance on black spruce wood.

Loss in adhesion (percentage) during the accelerated aging treatment was statistically influenced by rake angle. This loss in adhesion was lower than that observed for sanded samples (Cool and Hernández 2011c). Loss in adhesion was lower for samples prepared with rake angles of 10° and 20° (Table 5). Thus, a surface characterized by low subsurface damage and a certain level of fibrillation could favor adhesion of the studied waterborne coating. As reported by Cool and Hernández (2011a), when gluing

Table 5.—Loss in adhesion of a waterborne interior coating applied on black spruce wood specimens prepared by peripheral planing at three different rake angles.[a]

Rake angle (°)[b]	Loss in adhesion (%)
10	19 A
15	25 B
20	22 AB

[a] Values are means of 90 replicates. Means followed by the same letter are not significantly different at the 5 percent probability level.
[b] Feed speed values pooled.

planed black spruce wood, it seems that low cellular damage prevented degradation of the wood-coating interface and that fibrillation level observed was sufficient to enhance mechanical anchorage. Surfaces planed with a rake angle of 10° did not present torn grain and were defined by higher surface roughness (Table 1) and lower surface energy (Tables 2 and 3), which was constant for the three studied wavelengths. On the other hand, quality of surfaces planed with a 20° rake angle was influenced by wavelength, and the surfaces were characterized by torn grain, lower surface roughness, and higher surface energy. Therefore, chemical adhesion could be as important as the mechanical adhesion depending on cutting parameters.

According to our results, a rake angle of 10° at a wavelength of 1.3 mm is recommended, because it produced surfaces characterized by little torn grain and good initial pull-off strength and low loss in adhesion during accelerated aging. Compared with a rake angle of 20° that induced a similar loss in adhesion, cutting forces should be more important. Because the clearance angle was constant for all rake angles, the knife angle was higher for a 10° rake angle and should compensate for the higher wear rate that could be expected at lower rake angles. Furthermore, samples planed with a rake angle of 20° induced torn grain when feed speed was superior to 0.8-mm wavelength. Hence, the use of a rake angle of 10° with a wavelength of 1.3 mm (13 m/min feed speed) would be appropriate.

Conclusions and Recommendations

Rake angle and feed speed during peripheral planing of black spruce wood had a significant impact on anatomy, roughness, and energy of surface. Rake angle and feed speed both affected chip formation and surface characteristics at

Table 4.—Pull-off strength, before and after an accelerated aging treatment, of a waterborne interior coating applied on black spruce wood specimens prepared by planing at three rake angles and wavelengths.[a]

Rake angle (°)	Wavelength (mm)	Before aging (MPa)	After aging (MPa)	Loss in adhesion (%)
10	0.8	4.1 (0.2) BCD	3.3 (0.1)	19
	1.0	3.7 (0.2) D	3.3 (0.1)	12
	1.3	4.6 (0.2) A	3.4 (0.2)	25
15	0.8	3.9 (0.1) CD	3.3 (0.2)	16
	1.0	4.5 (0.1) AB	3.1 (0.1)	30
	1.3	4.6 (0.1) A	3.3 (0.1)	29
20	0.8	4.3 (0.1) ABC	3.5 (0.1)	19
	1.0	4.0 (0.2) CD	3.1 (0.1)	22
	1.3	4.0 (0.2) CD	3.0 (0.1)	25

[a] Values are means (standard errors of the means) of 30 replicates. Means followed by the same letter are not significantly different at the 5 percent probability level.

the microscopic level, surface roughness and surface energy. Samples machined with a rake angle of 10° lost less pull-off strength during the accelerated aging treatment. However, detected differences were negligible within the range of wavelength studied. Because feed speed did not have a significant effect on loss in adhesion, a feed speed of 13 m/min (1.3-mm wavelength) could be used to increase productivity. Furthermore, in opposition to samples planed with a 20° rake angle, a rake angle of 10° did not show torn grain on surfaces. In addition, these surfaces were characterized by low subsurface damage as well as an appropriate level of fibrillation to increase surface roughness and mechanical anchorage. Although wear can affect the surface topography at the microscopic and macroscopic level and can considerably modify wetting properties and pull-off strength, the effect of tool wear was not evaluated in this study. Consequently, in future research, it would be interesting to account for tool wear and quantify its impact on surface quality and coating adhesion. No correlations were obtained between surface quality parameters and pull-off tests, which indicates that the latter are required in assessing coating performance of black spruce surfaces.

Acknowledgments

The authors thank Luc Germain, Daniel Bourgault, Benoit Harbour, and Dany Bourque for valuable assistance, as well as Renaud Gilbert from Société Laurentide. This research was supported by the ForValueNet–NSERC strategic network on forest management for value-added products.

Literature Cited

American Society for Testing and Materials (ASTM). 1998. Standard test method for humid-dry cycling for coatings on wood and wood products. ASTM D3459. ASTM, Philadelphia.

Ashby, M. F., K. E. Easterling, R. Harrysson, and S. K. Maiti. 1985. The fracture and toughness of woods. *Proc. R. Soc. Lond. Ser. A Math Phys. Sci*. 398(1815):261–280.

ASTM International. 2002. Standard test method for pull-off strength of coatings using portable adhesion testers. ASTM D4541. ASTM, Philadelphia.

ASTM International. 2004. Standard methods for conducting machining tests of wood and wood base materials. ASTM D1666. ASTM, Philadelphia.

Cantin, M. 1967. Propriétés d'usinage de 16 essences de bois de l'Est du Canada. Publication No. 1111S. Direction générale des forêts, Canada. 31 pp.

Carrano, A. L., J. B. Taylor, and R. Lemaster. 2004. Machining-induced subsurface damage of wood. *Forest Prod. J*. 54(1):85–91.

Cool, J. and R. E. Hernández. 2011a. Evaluation of four surfacing methods on black spruce wood in relation to poly (vinyl acetate) gluing performance. *Wood Fiber Sci*. 43(2):194–205.

Cool, J. and R. E. Hernández. 2011b. Performance of three alternative surfacing processes on black spruce wood surfaces in relation to water-based coating adhesion. *Wood Fiber Sci*. 43(4):365–378.

Cool, J. and R. E. Hernández. 2011c. Improving the sanding process of black spruce wood for surface quality and water-based coating adhesion. *Forest Prod. J*. 61(5):372–380.

de Meijer, M., S. Haemers, W. Cobben, and H. Militz. 2000. Surface energy determination of wood: Comparison of methods and wood species. *Langmuir* 16(24):9352–9359.

de Moura, L. F., J. Cool, and R. E. Hernández. 2010. Anatomical evaluation of wood surfaces produced by oblique cutting and face milling. *IAWA J*. 31(1):77–88.

de Moura, L. F. and R. E. Hernández. 2005. Evaluation of varnish coating performance for two surfacing methods on sugar maple wood. *Wood Fiber Sci*. 37(2):355–366.

de Moura, L. F. and R. E. Hernández. 2007. Characteristics of sugar maple wood surfaces machined with the fixed-oblique-knife pressure-bar cutting system. *Wood Sci. Technol*. 41(1):17–29.

Fujiwara, Y., Y. Fujii, and S. Okumura. 2005. Relationship between roughness parameters based on material ratio curve and tactile roughness for sanded surfaces of two hardwoods. *J. Wood Sci*. 51(3):274–277.

Gardner, D. J., N. C. Generalla, D. W. Gunnells, and M. P. Wolcott. 1991. Dynamic wettability of wood. *Langmuir* 7(11):2498–2502.

Gindl, M., A. Reiterer, G. Sinn, and S. E. Stanzl-Tschegg. 2004. Effects of surface ageing on wettability, surface chemistry, and adhesion of wood. *Holz Roh- Werkst*. 63(4):273–280.

Gurau, L., H. Mansfield-Williams, and M. Irle. 2005. Processing roughness of sanded wood surfaces. *Holz Roh- Werkst*. 63(1):43–52.

Hernández, R. E., C. Bustos, Y. Fortin, and J. Beaulieu. 2001. Wood machining properties of white spruce from plantation forests. *Forest Prod. J*. 51(6):82–88.

Hernández, R. E. and L. F. de Moura. 2002. Effects of knife jointing and wear on the planed surface quality of northern red oak wood. *Wood Fiber Sci*. 34(4):540–552.

Hernández, R. E. and N. Naderi. 2001. Effect of knife jointing on the gluing properties of wood. *Wood Fiber Sci*. 33(2):292–301.

Hernández, R. E. and G. Rojas. 2002. Effects of knife jointing and wear on the planed surface quality of sugar maple wood. *Wood Fiber Sci*. 34(2):292–305.

International Organization for Standardization (ISO). 1996. Geometrical product specifications (GPS). Surface texture. Profile method; Surfaces having stratified functional properties. Part 2: Height characterisation using the linear material ratio curve. ISO 13565-2. ISO, London.

International Organization for Standardization (ISO). 1997. Geometrical product specifications (GPS). Surface texture. Profile method. Terms. Definitions and surface texture parameters. ISO 4287. ISO, London.

International Organization for Standardization (ISO). 2002. Geometrical product specifications (GPS)—Filtration part 31: Robust profile filters. Gaussian regression filters. ISO 16610-31. ISO, London.

Iskra, P. and R. E. Hernández. 2012. Analysis of cutting forces in straight-knife peripheral cutting of wood. *Wood Fiber Sci*. 44(2):134–144.

Jessome, A. P. 1977. Résistance et propriétés connexes des bois indigènes au Canada. Rapport technique de foresterie 21. Laboratoire des produits forestiers de l'Est, Ottawa. 37 pp.

Koch, P. 1972. Utilization of the southern pines. Volume 2—Processing. Agriculture Handbook. USDA Forest Service, Washington, D.C. 1,663 pp.

Koch, P. 1985. Utilization of hardwoods growing on southern pine sites. Volume II—Processing. Agriculture Handbook No. 605. USDA Forest Service, Washington, D.C. 3,710 pp.

Lihra, T. and S. Ganev. 1999. Machining properties of eastern species and composite panels. Forintek Canada Corp., Division de l'Est, Sainte-Foy, Quebec, Canada. 62 pp.

Murmanis, L., B. H. River, and H. A. Stewart. 1983. Microscopy of abrasive-planed and knife-planed surfaces in wood-adhesive bonds. *Wood Fiber Sci*. 15(2):102–115.

Murmanis, L., B. H. River, and H. A. Stewart. 1986. Surface and subsurface characteristics related to abrasive-planing conditions. *Wood Fiber Sci*. 18(1):107–117.

Piao, C., J. E. Winandy, and T. F. Shupe. 2010. From hydrophilicity to hydrophobicity: A critical review: Part 1. Wettability and surface behaviour. *Wood Fiber Sci*. 42(4):490–510.

SAS Institute Inc. 2007. SAS/STAT Users' Guide, version 9.2. SAS Institute Inc., Cary, North Carolina.

Singh, A. P. and B. S. W. Dawson. 2004. Confocal microscope—A valuable tool for examining wood-coating interface. *J. Coatings Tech. Res*. 1(3):235–237.

Singh, A. P. and B. S. W. Dawson. 2006. Microscopic assessment of the effect of saw-textured pinus radiate plywood surface on the distribution of a film-forming acrylic stain. *J. Coatings Tech. Res*. 3(3):193–201.

Singh, A. P., B. S. W. Dawson, K. D. Hands, J. W. Ward, M. Greaves, J. C. P. Turner, and C. L. Rickard. 2010. The anatomy of raised grain on *Pinus radiata* weatherboards. *IAWA J*. 31(1):67–76.

Stewart, H. A. and J. B. Crist. 1982. SEM examination of subsurface

damage of wood after abrasive and knife planing. *Wood Sci*. 14(3):106–109.
Thay, P. D. and P. D. Evans. 1998. The adhesion of an acrylic primer to weathered radiata pine surfaces. *Wood Fiber Sci*. 30(2):198–204.
Wang, S., Y. Zhang, and C. Xing. 2007. Effect of drying method on the surface wettability of wood strands. *Holz Roh- Werkst*. 65:437–442.
Williams, D. and R. Morris. 1998. Machining and related mechanical properties of 15 B.C. wood species. Forintek Canada Corp., Western Division, Vancouver, British Columbia, Canada. 31 pp.
Wolkenhauer, A., G. Avramidis, Y. Cai, H. Militz, and W. Viöl. 2007. Investigation of wood and timber surface modification by dielectric barrier discharge at atmospheric pressure. *Plasma Process Polym*. 4(1):S470–S474.
Wu, S. 1971. Calculation of interfacial tension in polymer systems. *J. Polym. Sci. Part C* 34:19–30.